





Article

Study of a Hybrid Solar Absorption-Cooling and Flash-Desalination System

Nicolás Velázquez-Limón ¹, Ricardo López-Zavala ^{2,*} , Luis Hernández-Callejo ^{3,*} ,
Jesús A. Aguilar-Jiménez ¹ , Sara Ojeda-Benítez ²  and Juan Ríos-Arriola ¹ 

¹ Centro de Estudios de las Energías Renovables, Instituto de Ingeniería, Universidad Autónoma de Baja California, Mexicali 21280, Mexico; nicolas.velazquez@uabc.edu.mx (N.V.-L.); a1116072@uabc.edu.mx (J.A.A.-J.); riosj9@uabc.edu.mx (J.R.-A.)

² Laboratorio de Residuos Sólidos, Instituto de Ingeniería, Universidad Autónoma de Baja California, Mexicali 21280, Mexico; sara.ojeda.benitez@uabc.edu.mx

³ Department of Agricultural Engineering and Forestry, Campus Universitario Duques de Soria, University of Valladolid (UVA), 42004 Soria, Spain

* Correspondence: rlopez99@uabc.edu.mx (R.L.-Z.); luis.hernandez.callejo@uva.es (L.H.-C.)

Received: 27 June 2020; Accepted: 21 July 2020; Published: 1 August 2020



Abstract: In this work, the analysis of a hybrid LiBr/H₂O absorption-cooling and flash-desalination system, using solar thermal energy as heat source, is presented. An absorption open-cycle with three pressure levels is used in combination with a single-stage flash-desalination process to use the coolant as product water, resulting in an increase in cooling and desalination efficiency. For the application, a 20-room coastal hotel complex in San Felipe, Baja California, Mexico, is taken as a case study and the sizing of the solar collection and storage system is carried out for the operation of the proposed hybrid system, during the summer operative period. The operational dynamics during the week with the highest ambient temperatures are presented. The dimensioning of the solar collector's area and the energy storage resulted in a collection area of 620 m² with 30 m³, respectively, reaching a solar fraction of 69%. The absorption-cooling subprocess showed an increase of 13.88% in the average coefficient of performance (COP) compared to conventional LiBr/H₂O absorption systems. Also, considering that the system provides cooling and desalination simultaneously, the average COP_C is 1.64, which is 2.27 times higher than the COP of conventional LiBr/H₂O single-effect absorption units. During the critical week, the system presented a desalinated water production of 16.94 m³ with an average performance ratio (PR) of 0.83, while the average daily water production was 2406 kg/day; enough to satisfy the daily water requirements of four people in a coastal hotel in Mexico or to cover the basic services of 24 people according to the World Health Organization.

Keywords: solar energy; absorption cooling; desalination

1. Introduction

Future energy technologies must be designed to use clean and renewable sources of energy, as well as waste energy, in order to achieve sustainable development that ensures the well-being of the world's population. Energy generation systems need to consume less energy and be more efficient in order to reduce environmental pollution and increase their profitability.

The increase in population has brought with it a substantial increase in the demand for energy to meet basic needs, such as air conditioning and access to drinking water. In the United States alone, 10% of total annual energy consumption in 2019 was used for space cooling in buildings, equivalent to 380 billion kWh [1], while in other developed countries 30% of the energy produced is consumed by heating, ventilation, and air conditioning systems (HVAC) [2].

On the other hand, seawater desalination is one of the main methods for meeting the needs for drinking water in regions where it is difficult to acquire it by other means [3,4]. For this purpose, there are different technologies, such as multiple-effect desalination (MED), multi-stage flash (MSF), humidification-dehumidification (HDH), reverse osmosis (RO), membrane distillation (MD), among others, that are widely used and with a high level of technological development. However, at present the energy cost of desalinating water is considerably high [5] and, if fossil fuels are used as energy sources, the environmental pollution generated by water desalination is harmful [6]. Renewable energies are a sustainable option to generate the energy required by this type of system, eliminating the problem of pollution and with competitive costs [7–9].

In recent years, great efforts have been made to integrate renewable energies into desalination processes [10] and space cooling [11], and clearly there is a wide use of solar energy, both thermal and photovoltaic, to produce both services in a sustainable way [12,13]. Within desalination, solar thermal energy has been successfully used in MED, MSF, MD, and HDH systems [14], while photovoltaic is undoubtedly an excellent option for RO [15]. This is mainly because there is a relationship between water scarcity and the availability of solar radiation in many regions [16]. On the other hand, absorption-cooling systems are efficiently coupled with solar heating technologies in regions with difficult access to electricity [17,18]. Currently, the trend is in the hybridization of technologies, seeking greater efficiency and less pollution [19], performing energy and mass integrations between the different streams.

Anand & Murugavelh [20] studied a vapor refrigeration system operating with an HDH system for fresh water production. The results mention that the energy consumption may decrease and the cooling capacity increase when the ambient temperature tends to decrease, while at high ambient temperature the water desalination system is seen to benefit, but the cooling capacity is negatively affected. However, in this study the activation energy came from the combustion of fossil fuels. In turn, Qasem et al. [21] analyzed the integration between an HDH desalination system and an absorption-cooling system. The seawater from the HDH is used as a heat removal medium from the absorber and condenser of the cooling system, acquiring sufficient energy to activate the HDH. The optimal cooling capacity was 62 tons and a water production of 1145 L/h. Its results show a 2.2-times improvement in HDH efficiency and an 8.24-times reduction in the cost of fresh water compared to traditional HDH systems. The HDH desalination systems are attractive in low water demand and cooling applications; however, they are severely limited by climatic conditions, especially high levels of air humidity, so their use in large coastal buildings may not be suitable. Another very interesting energy integration is to use the heat of condensation from a power cycle to activate desalination and absorption thermal systems. Kerme et al. [22] analyzed a system for desalination, power generation, and cooling using solar energy. This system consists of a parabolic trough solar concentrator field that generates the thermal energy to activate an organic Rankine cycle, which, in turn, uses the heat of condensation from the working fluid to activate a MED system and an absorption system. With this energy integration it is possible to reduce the thermal energy requirements of process activation.

In India, Sahoo et al. [23] presented a theoretical study of a polygenerative system that produces electrical energy, water, and cooling. A power cycle of steam activated with solar thermal energy and biomass was proposed, where the steam coming out of the turbine is used to activate the first effect of a LiBr/H₂O double-effect absorption-cooling unit, while the heat of condensation from the absorption system is used for the activation of an HDH desalination process. To activate the system, a parabolic trough collector field with an aperture area of 31,339 m² and a biomass system with a capacity of 17.4 MJ/kg were used. A cooling coefficient of performance (COP) of 1.42 was reported, with a cooling capacity of 2805.5 kW and a freshwater desalination of 900 L/h. However, the coupling of these technologies involves a large number of components, increasing the initial investment. Alelyani et al. [24] proposed novel integrations between absorption-cooling systems and MED desalination systems, where the heat from the condenser and absorption rectifier equipment is used to thermally activate the MED in the first effect. Their results show that with the proposed

integration cost of water production increases by 9% with respect to a MED without integration, but with a reduction of 42% in the cost of cooling production. Mohammadi & McGowan [25] analyzed the integration of an absorption and vapor compression cooling system with a MED system and found that the desalination system produces an appreciable amount of water using the steam discarded by the absorption-cooling cycle.

Different authors have studied the application of hybrid systems that include space cooling and desalination in isolated regions. Calise et al. [26] proposed a polygenerative system based on solar energy and biomass to meet the needs of cooling, seawater desalination, heating, and electricity of an isolated small community. In another study, Calise et al. [27] made a modification to their previous system and analyzed it under typical operating conditions of a building on Pantelleria Island. Recently, a solar thermal activated polygenerative process was proposed to provide electrical power, fresh water, and space cooling to a hotel in Eastern Azerbaijan, Iran [28]. In this system, it is proposed to use a Stirling solar dish activated with solar thermal energy to generate electricity for the building; in addition, to activate the HDH desalination process, the heat rejected by the Stirling engine is used and, for space cooling, a vacuum vessel is used to cool a closed air system. On a typical day, the temperature inside the building was 25 °C; the maximum efficiency of the solar Stirling engine was 36.3% and the electrical power output was 38.8 kW. The maximum activation energy was reported to be 97.12 kW, with a cooling capacity of 229 kW and a Gained Output Ratio (GOR) of 2.35. However, controlling the generation of electrical energy in this system is complex and the initial investment may be high.

In the works mentioned above, a trend can be appreciated in proposing systems that produce different services in a more efficient and sustainable way. The hybridization and energy integration of technologies has reduced energy consumption by taking advantage of the waste heat among them. However, it is necessary to continue improving the current technologies, seeking a better energy and mass integration that allows a decrease in energy consumption, as well as in the system components, making use of renewable energy sources available at the project location. Following the global efforts, this paper presents a novel hybrid LiBr/H₂O absorption-cooling and seawater flash-desalination system that uses solar thermal energy as a heat source. This system couples a single-effect absorption-cooling open-cycle with three pressure levels, thus allowing an internal energy and mass integration with a single-stage flash-desalination process. The activation temperature levels are suitable to enable the system to be coupled to a solar thermal collector field to obtain the energy required for its operation. This system is an improvement to the work presented in [29] and is studied under the dynamics of solar resource availability and cooling demand variation of a 20-room hotel complex as a case study.

The description of the hybrid system, as well as the process of cooling and thermosolar desalination, is presented in Section 2. It also mentions the methodology used to carry out the study, defining the simulation considerations and describing the characteristics of the case study, such as its meteorological conditions that affect the operation of the system and the calculation of the cooling demand. Section 3 shows the results of the energy-operating analysis of the hybrid system during the summer period and during one week with the highest environmental temperatures of the year, where both cooling and water desalination performances can be appreciated. Finally, the most important conclusions are presented in Section 4.

2. Materials and Methods

2.1. System Description

The proposed system consists of the coupling of a LiBr/H₂O single-effect absorption-cooling open-cycle that has three levels of pressure, with a one-stage flash-desalination process. The system is divided into four subprocesses: (1) the cooling subprocess; (2) the desalination subprocess; (3) the product water extraction and conditioning subprocess, and (4) the solar thermal energy collection and storage subprocess, which are shown in Figure 1.

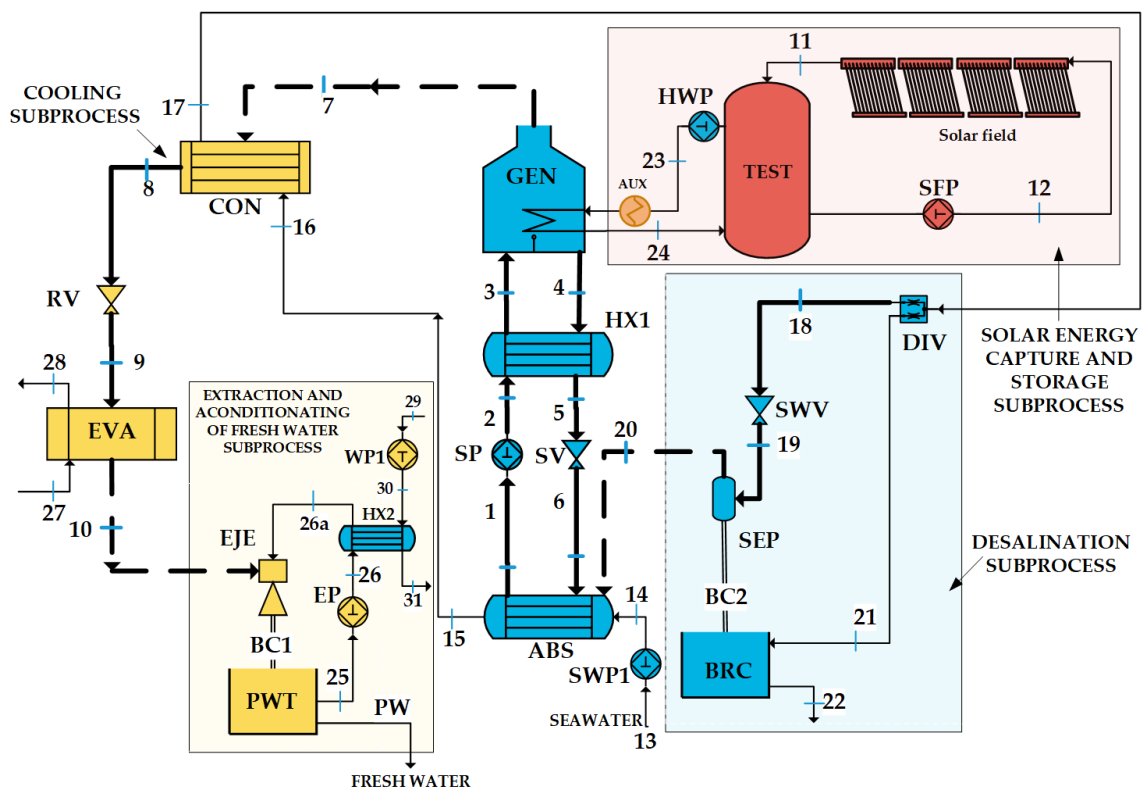


Figure 1. Schematic diagram of hybrid solar absorption-cooling and flash-desalination system.

In the cooling subprocess, the hot water flow (23) coming from the solar thermal energy collection and storage subprocess enters the generator (GEN) to heat the weak solution $\text{LiBr}/\text{H}_2\text{O}$ flow (3), producing the separation of water vapor (7). The vapor (7) is taken to the condenser (CON), to undergo a phase change by exchanging latent heat with the seawater stream (16) and leave as a saturated liquid (stream 8). On the other hand, the strong solution (stream 4) exchanges sensitive heat with the stream (2) of diluted solution, in order to bring both streams closer to the process of desorption and absorption, respectively. The stream (4) after decreasing its temperature, leaves the HX1 as the stream (5) and is taken to a solution expansion valve (SV). When leaving this valve, the stream (6) decreases its pressure and in these conditions enters the absorption equipment (ABS). In the absorber, the stream (6) absorbs water vapor (20) from the desalination subprocess, producing an exothermic reaction. The pump (SWP) suction in the seawater stream (13) and conducts it as stream 14 to dissipate the heat of the exothermic reaction in the absorber and leaves at a higher temperature (stream 15 = 16) and is conducted to condense the steam (7) produced in the GEN. The stream (17), after receiving the condensation heat, leaves the condenser and enters the desalination subprocess and is taken to a stream divider (DIV), where it is divided into streams (18) and (21). The stream (21) is taken to a brine dilution vessel (BRC); while the stream (18) goes through an expansion process, so it flashes, due to the pressure decrease, and remains in two phases (stream 19). The two-phase stream (19) enters a liquid-vapor separator (SEP); here the vapor is separated (20) and taken to the cooling subprocess to enter the ABS and be absorbed. On the other hand, the liquid brine leaving the SEP is taken to a barometric column (BC2) and, then, exits to the BRC; the function of the barometric column (BC2) is to serve as a hydraulic seal by maintaining the vacuum pressure and allowing the brine to be raised to atmospheric pressure.

In the cooling subprocess, the liquid coolant (8) passes through an expansion valve (VR) producing a slight flash, caused by the decrease of its pressure and temperature (stream 9); in these conditions, it enters the evaporator (EVA) to produce the cooling effect. The cooling water (27) enters to the evaporator equipment and is cooled, causing the refrigerant (10) to change its state at the exit of the

evaporator and leave as saturated steam; in these conditions the stream (10) enters to the expansion and product water conditioning subprocess.

In the subprocess of extraction and adaptation of product water, the current (10) after the cooling effect in the EVA is suctioned by the ejector unit (EJE), which is activated with the driving fluid (26) coming out of the cooler (HX2). The low pressure vapor stream 10 is mixed with the high-pressure liquid stream (26), both mixed fluids are compressed by the ejector diffuser, at a pressure intermediate between the pressures of streams (10) and (26); this pressure has the appropriate value for vapor 10 to condense, while the liquid stream (26) receives this condensation heat. This causes both streams, now in liquid phase, to increase their temperature at the outlet of the ejector diffuser. The liquid stream leaving the ejector is discharged into the barometric column (BC1), which allows the vacuum to be maintained in the system and the water leaving the ejector to be deposited in the product water tank. The stream (25) is suctioned by the pump (EP) and is taken (stream 26) to dissipate the heat of condensation in the cooling equipment (HX2); the stream 26a coming out of HX2, is again able to receive the heat of condensation from the steam 10.

It is important to note that the hybrid system uses three pressure levels where the absorber has a higher pressure than the evaporator, which results in a thermal compressor with less ΔP , improving efficiency and allowing the evaporator to work with adequate pressures for cooling [29]. On the other hand, the system has an internal energy integration in which the heat from the absorber and condenser is used to preheat the seawater before it is taken to the desalination subprocess; this allows the cooling of the CON and ABS without requiring an expensive cooling tower. Finally, to condense the cooling steam, barometric ejecto-condensers are used, which are passive elements that allow maintaining the vacuum in the system, besides compressing the cooling steam until it is condensed, without a high energy cost.

The solar thermal energy collection and storage subprocess convert solar radiation into high quality thermal energy, which is used to drive the hybrid system's generator. During the day, water is taken from the bottom of the thermal energy storage tank (TEST) to be conducted to the solar collector field through the stream (12); the collectors are connected in a series and parallel arrangement to ensure the temperature level and amount of energy required for the operation of the system. As long as there is enough solar radiation to raise the temperature of the stream (11) above that of the stream (12), the solar fluid pump (SFP) will remain on. During operation of the hybrid system, energy is extracted at the rate of the cooling demand by the stream (23) and the HWP, resulting in nonconstant conditions within the TEST. The solar collectors in a certain period of heating will be supplying the amount of energy sufficient for the operation of the hybrid system and, also, for storage in sensible heat form within the TEST for the periods of null (night) or low solar radiation. If the temperature of the stream (23) falls below 78 °C because the stored energy and/or the energy produced by the collector field is not sufficient to meet the demand, the auxiliary heater (AUX) shall be used to reach the minimum operating temperature.

Table 1 shows the characteristics of the equipment used in the study. The capacity of the equipment is analyzed below.

Table 1. System characteristics.

Hybrid Cooling-Absorption and Flash-Desalination System	
Max. cooling capacity	80 kW
Min. cooling capacity	16 kW
Mass flow activation m_{11}	5.62 kg/s
Temp. of seawater (stream 13)	27 °C
Mass flow of seawater (stream 13)	3.39 kg/s
Evaporator temp.	6 °C
Condenser temp.	34.30 °C
Absorber temp. (stream 1)	32 °C
Inlet chiller temp.	12 °C
Flow solution	0.28 kg/s
Solar Collector	
Brand/model	Suntask/SHC24
Collector type	Evacuated tube with CPC reflector
Number of tubes	24
Aperture area	4.41 m ²
Optical efficiency (a0)	0.668
First order efficiency coefficient (a1)	1.496 W/m ² °C
Second order efficiency coefficient (a2)	0.005 W/m ² °C ²
Fluid	Water
Mass flow	0.02 kg/s m ²
Thermal Energy Storage Tank	
Material	Fiberglass
Insulation thickness	0.025 m
Loss coefficient	1.4 W/m ² K
Fluid	Water

2.2. Methods

The simulation of the hybrid system activated with solar thermal energy was carried out by means of three software:

1. Aspen Plus was used to evaluate the internal operation of the absorption-cooling and flash-desalination system.
2. Through the TRNSYS software, the thermal load and capacity of the solar thermal collector and TEST system were determined.
3. MATLAB was used to evaluate the coupling of the solar thermal collector, TEST, and thermal load with the proposed hybrid system.

The considerations for making the operational study are presented below:

- The proposed cycle operates in stable conditions. The LiBr/H₂O solution is homogeneous and in balance. The weak solution is at 51%.
- The steam (22) generated in sudden evaporation must be equal to the steam (7) produced in the GEN.
- Operating pressures were set as reported in [29], unless otherwise mentioned.
- The maximum operating cooling capacity was set at 80 kW, and a minimum partial load operation of 20% (16 kW).
- The approach temperatures of the heat exchanger equipment EVA, GEN, ABS, CON and HX1 are those reported by [29] and those of HX2 are those reported by [30].
- The design flows of the external system circuits were considered according to the AHRI standard [31]. Seawater was considered to have a concentration of 35,000 ppm with a temperature of 27 °C, as reported by [32] and the composition based on [33].

- The minimum operating temperature of the hybrid system is 78 °C; a lower temperature will force the use of the auxiliary heater.
- The on/off switching of the solar field pump was controlled by temperature difference ($[T_{out} - T_{in}] > 0$).
- 30-min simulation intervals.

Figure 2 shows the methodology and simulation process used in this study.

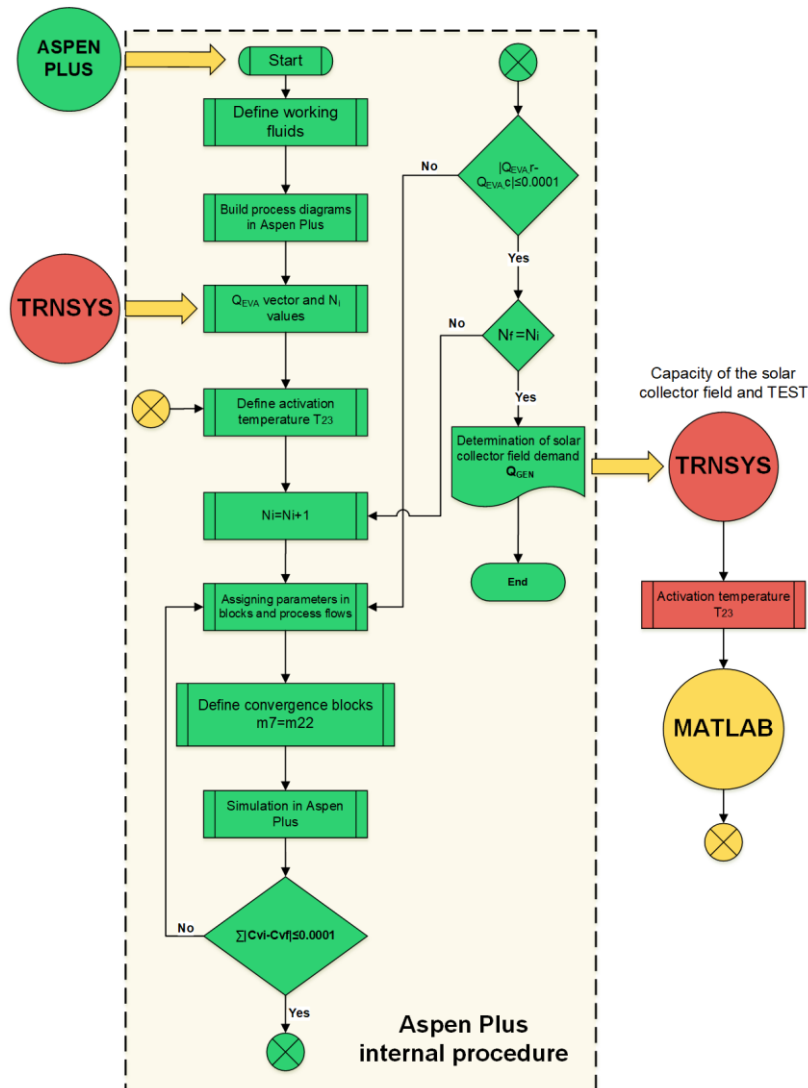


Figure 2. Methodology and software simulation procedure.

2.3. System Simulator Validation

Validation of the system simulator was done using Aspen Plus software; this is specialized software for chemical, heat transfer, and mass process analysis. Aspen Plus has thermodynamic properties of many working fluids already validated and with experimental correlations on the operation of various industrial equipment. The validation of the proposed system was done in two parts, where the absorption-cooling subprocess was validated, with the experimental results reported by Florides et al. [34] and the flash-desalination subprocess with the results reported by Kahraman & Cengel [35] and Palenzuela et al. [36].

After performing the validation study for both subprocesses, it was found that the largest deviation was presented with the experimental results of Florides et al. and did not exceed 3%, so it can be

concluded that Aspen Plus is a good option to study the operability of the system. The validation can be verified in the work of López-Zavala et al. [29].

2.4. Case Study

To operatively study the technological proposal influenced by real operating conditions, a 20-room hotel complex located in the city of San Felipe, Baja California, Mexico ($31^{\circ}01'22.1''$ N $114^{\circ}49'56.5''$ W) was taken as a case study. This city is characterized by its coastal location, with a high level of tourism and high environmental temperatures during the summer, which can reach 45°C in the shade. It presents difficulty in accessing drinking water, its main source being the waters coming from the Colorado River that are transported from Mexicali, which is approximately 200 km away. However, San Felipe has an excellent solar resource for its energy exploitation, so this location is suitable for analyzing the proposal.

The calculation of the cooling demand was made with the Type 56 (TRNBuild) of TRNSYS, an interior temperature of 25°C was established during 24 h of the day for a building formed by concrete blocks ($k = 1.64\text{ w/m}^{\circ}\text{C}$, $\rho = 2011\text{ kg/m}^3$, $C_p = 0.91\text{ kJ/kg}^{\circ}\text{C}$) that were 8 m long, 7.5 m wide, and 2.75 m high. Thermal gains generated by four people performing resting activities (480 W), artificial lighting (75 W), and a television (60 W) were considered. Figure 3 shows the profiles of (a) ambient temperature, (b) global radiation, and (c) cooling demand and daily mean ambient temperature of the hotel complex during the June–September period, considering the months with the highest tourist affluence and high ambient temperatures.

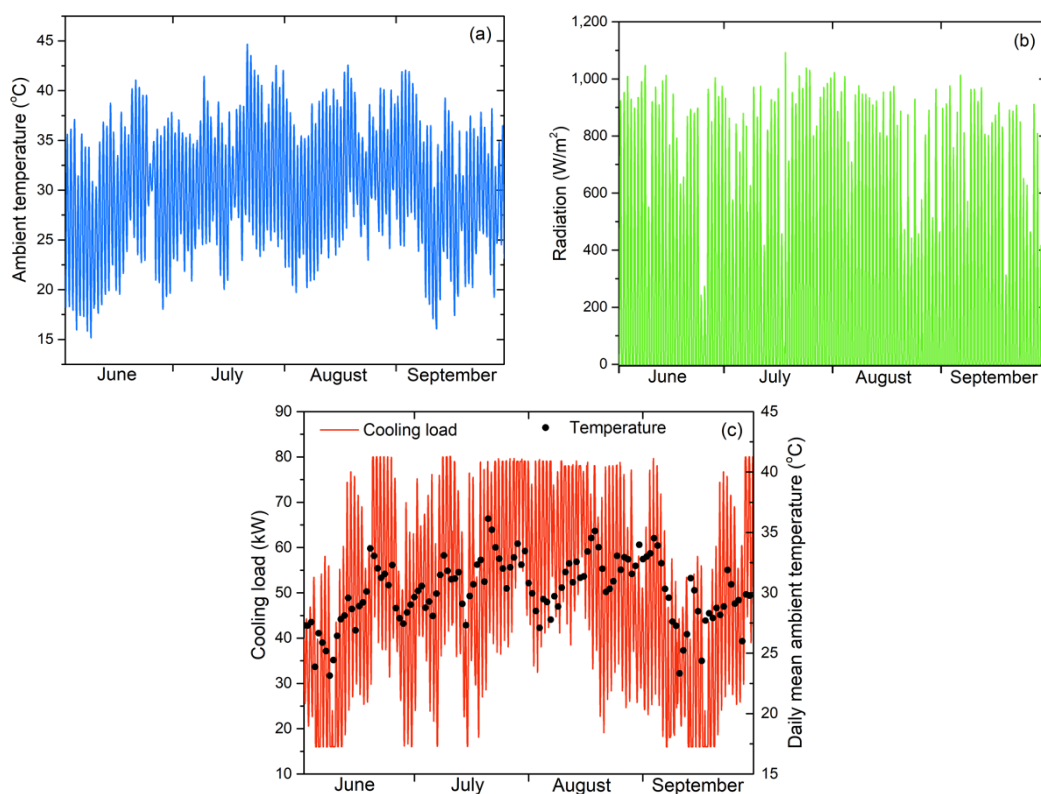


Figure 3. Profile of (a) ambient temperature, (b) global radiation, and (c) cooling demand and daily mean ambient temperature used in the simulation of the solar cooling and desalination system.

2.5. System Evaluation

The absorption system is evaluated with the COP indicator, which represents the ratio of the desired effect to the energy cost of producing it, according to Equation (1). Q_{EVA} is the cooling capacity, Q_{GEN} is the heat supplied to the system, SP is the solution pump power, W_{SWP} and W_{SWP1} represent

the work of the ABS and HX2 cooling pumps, respectively, and W_{EP} is the work of the ejector fluid pump. However, considering that this system produces fresh water and space cooling simultaneously, with the same main source of energy, a COP_G is proposed in accordance with Lopez-Zavala et al.'s proposal [30], calculated as shown in Equation (2), where m_{10} is the product water flow:

$$COP = \frac{Q_{EVA}}{Q_{GEN} + W_{SP} + W_{SWP} + W_{SWP1} + W_{EP}} \quad (1)$$

$$COP_G = \frac{Q_{EVA} + m_{10} \times \left(2326 \frac{kJ}{kg}\right)}{Q_{EVA}} \quad (2)$$

To evaluate desalination, the performance ratio (PR) indicator is used, which relates the amount of water produced in terms of energy with respect to the main activation energy of the desalination process [37], and is calculated with Equation (3):

$$PR = \frac{m_{10} \times \left(2326 \frac{kJ}{kg}\right)}{Q_{GEN}} \quad (3)$$

The thermal efficiency of solar collectors, $E_{f_{sf}}$, is evaluated based on Equation (4), as well as the heat contributed by each of the collectors, Q_{sf} , with Equation (5):

$$E_{f_{sf}} = a_0 - a_1 \frac{T_{in} - T_a}{G_T} - a_2 \frac{(T_{in} - T_a)^2}{G_T} \quad (4)$$

$$Q_{sf} = A_{SC} G_T E_{f_{sf}} \quad (5)$$

where a_0 , a_1 , and a_2 are the optical efficiency of the solar collector and the first and second order efficiency coefficient, respectively. T_{in} corresponds to the collector inlet temperature, T_a the ambient temperature, G_T the incident solar radiation in the collector aperture area, and A_{SC} the solar collection area.

The solar fraction represents the thermal energy contribution of the solar field and TEST to the hybrid system consumption and is calculated based on the Equation (6):

$$f_{sf} = \frac{\dot{Q}_{GEN} - \dot{Q}_{aux}}{\dot{Q}_{GEN}} \quad (6)$$

where \dot{Q}_{GEN} is the thermal energy required to meet the needs of the hybrid system and \dot{Q}_{aux} is the extra energy supplied by the auxiliary heater after the solar contribution to meet the demand for cooling and desalination.

3. Results

3.1. Analysis in Summer Period

In order to carry out a specific operational study of the system, it is necessary to determine the capacity of the solar collector area and the size of the TEST to satisfy the activation energy requirements throughout the operational period considered in the summer months. For such situation, an operational parametric analysis was performed during June–September using the meteorological conditions of the region and the load profile presented in Figure 3. The results on different variables are presented in Figure 4. Figure 4a analyzes the amount of auxiliary energy required to meet the thermal energy requirements of the cooling and desalination system. It can be seen how a low-capacity solar thermal collector field has no influence on the decrease in auxiliary energy consumption, regardless of the size of the TEST. From the 500 m² of solar collector area the volume of the TEST begins to have a positive effect; this is because the solar energy generated, as shown in Figure 4b, is sufficient to cause

an increase in the temperature of the water stored in the TEST and can be used to activate the hybrid system. From 600 m² onwards, there is a noticeable decrease in the auxiliary energy requirements and a greater effect of the size of the TEST. The aim of this parametric study is to find the appropriate size of the solar collector field, so Figure 4c shows the effect of these values on the cost of auxiliary energy and Figure 4d the solar fraction achieved. By increasing from 460 to 620 m², corresponding to a 25% increase in collector area, a 28% reduction in consumption and cost of auxiliary energy is achieved, while the solar fraction increases from 57% to 69%. However, increasing the capacity of the solar field by 20% and reaching 770 m² represents only a 7% increase in the solar fraction. Therefore, a capacity of 620 m² in the solar collector area and a TEST of 30 m³ was selected to carry out the operational study of the hybrid cooling and desalination system, which achieves a solar fraction of 69%, requiring an extra 53 MWh of auxiliary energy to satisfy the thermal energy requirements.

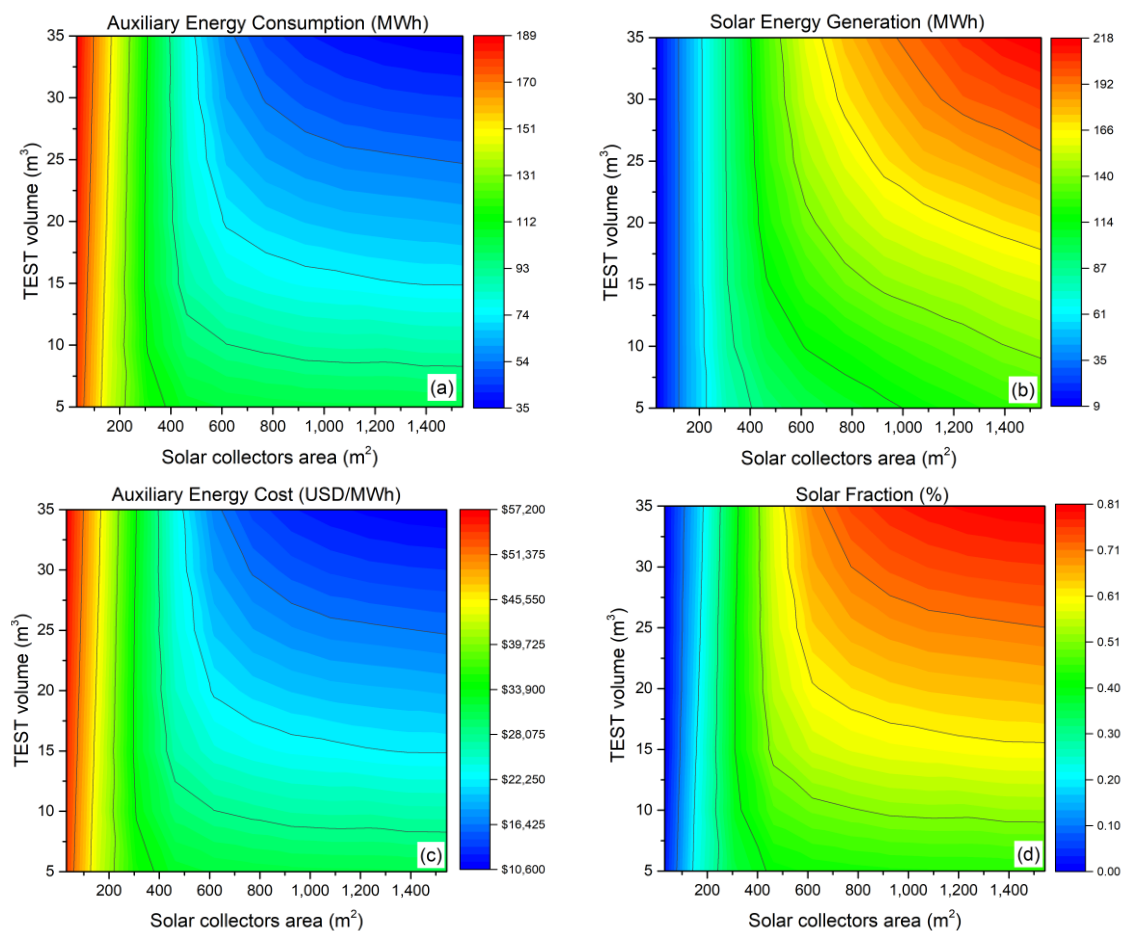


Figure 4. Effect of total solar collector area and total volume of the TEST on (a) auxiliary energy consumption, (b) solar energy generation, (c) auxiliary energy cost, and (d) solar fraction. A fuel cost of \$1.15 USD/L and an equivalence of 1 L = 3.79 kWh were considered, considering a conversion efficiency of 38%.

With the above, Figure 5 shows the energy accumulation generated or consumed by the solar collector field, the cooling and desalination system, and the auxiliary equipment. During the first weeks of June, when the cooling load is not so high, the solar energy and thermal storage capacity is sufficient to meet the energy requirements of the hybrid system. However, as time passes, the cooling load increases and the solar energy is no longer sufficient to cover the heat demand, especially for night periods, so the use of the auxiliary heater is required. During the four summer months analyzed, a total of 183 MWh of thermal energy was required to activate the cooling and desalination system, while the solar field and the auxiliary heater generated a total of 153 and 60 MWh, respectively. Approximately

31 MWh of solar thermal energy is lost due to energy storage capacity and the time lag between the cooling load and solar generation.

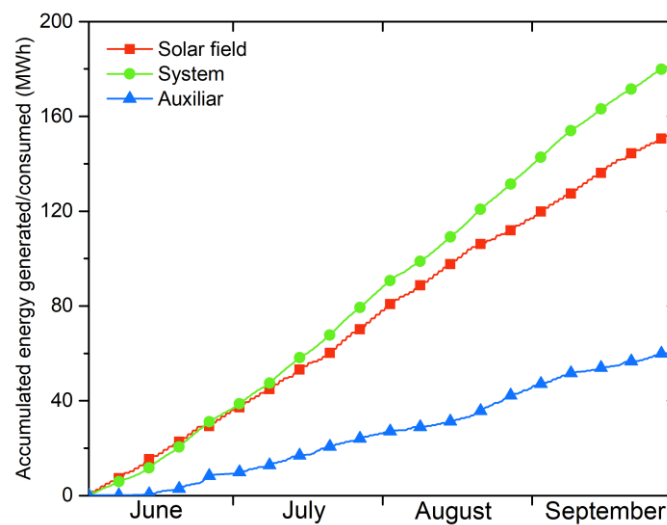


Figure 5. Accumulated energy generated or consumed by the solar field, cooling and desalination system, and auxiliary generator.

3.2. Weekly Operation

In order to further explore the operation of the solar hybrid system, the week of July 19–25 was selected because it has the highest ambient temperatures during the study period, reaching up to 45 °C in the shade. Figure 6 shows the behavior of the different temperatures that affect the system operation, as well as the horizontal global radiation. The average temperature dynamics of the TEST, as well as the temperature of the fluid entering the system's generator, can be seen. The stream entering the generator is taken from the top of the TEST, so it has a higher temperature than the average of the TEST. The minimum operating temperature of the cooling and desalination system is 78 °C, so during the day the solar field is sufficient to maintain the TEST temperature above this value. However, as the solar resource decreases, the tank also decreases its temperature due to the continuous extraction of energy, to the point that there is not enough solar energy to maintain the minimum operating temperature, so the auxiliary heater is used and has a constant temperature of 78 °C until the solar resource is sufficient to meet the heating demand.

The dynamics related to the heat generated by the solar collector field and the auxiliary heater, as well as that consumed by the generator, are shown in Figure 7. It can be seen that at the beginning of the week there is no solar resource stored in the TEST, so the auxiliary heater is responsible for satisfying the system's generator. As it is daytime and the solar radiation is sufficient to activate the generator, the auxiliary heater is stopped. During maximum solar exposure, the energy generated by the solar collectors is sufficient to meet the demand and store energy in the TEST. When solar power generation is completely finished, it can be seen that for a period of time energy continues to be supplied to the system's generator without the use of the auxiliary heater. This is because the TEST has sufficient quantity and quality of energy to keep the cooling and desalination system in operation. When the TEST temperature is below the minimum operating temperature, as shown in Figure 6, the auxiliary heater is turned on.

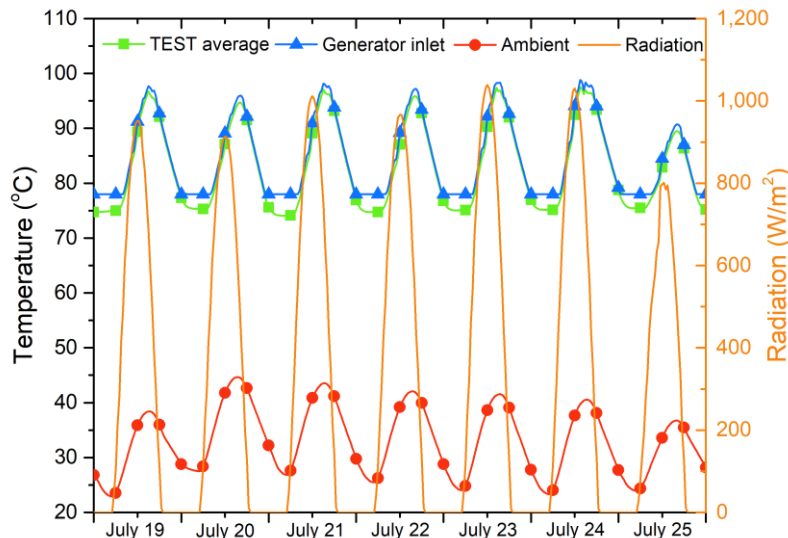


Figure 6. Variation of the average TEST temperature, system generator input temperature, and ambient temperature during an operational week.

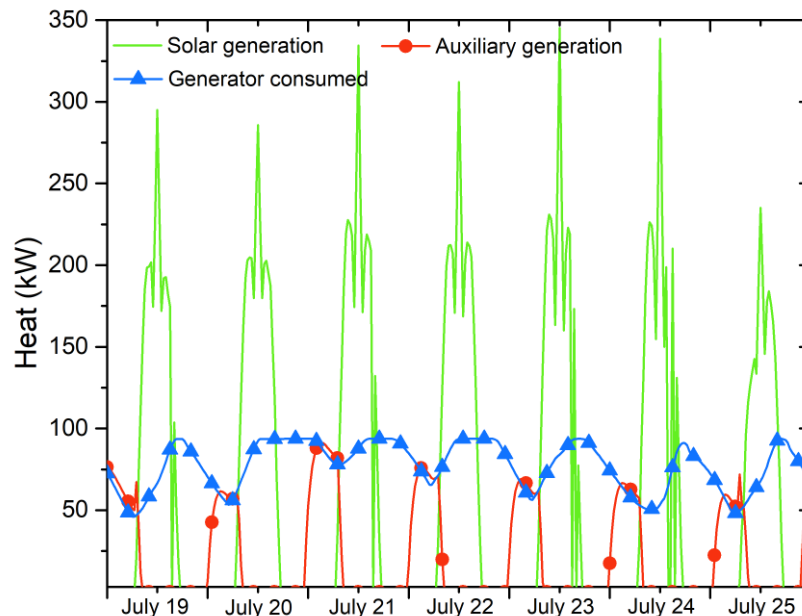


Figure 7. Variation in heat generation of the solar field and the auxiliary heater, and generator power consumption of the cooling and desalination system.

Figure 8 shows the heat transfer behavior of the GEN, EVA, CON, and ABS equipment of the system during the critical week of ambient temperature in summer. It can be seen that the increase in the cooling capacity causes an equal increase in the other heat-exchanger equipment. This is due to the fact that the cooling capacity is controlled by manipulating the addition of heat in the GEN; that is, when Q_{EVA} increases it is necessary to transfer more refrigerant fluid (7) to the evaporator, so the heat in the GEN increases. Furthermore, this vapor, needing to condense to go to the refrigerant expansion valve (VR), causes the increase of heat transfer in the CON. It is important to highlight that the steam flow (7) has to be equal to the steam (20) produced in the desalination subprocess to keep the thermal compressor in stable conditions and avoid possible crystallization problems. If the vapor (7) produced in the GEN is greater than the vapor (20), it will cause crystallization to occur and, if the vapor (7) is less than the vapor (20), then there would be an accumulation of mass in the absorption system, resulting in a change in pressure levels. To maintain the equality between the currents (7) and (20), the current divider (DIV) is used, in order to manipulate the flow of the current 19 and only use the sea

water necessary for the production of the steam (20); consequently, the increase of the steam (7) causes an increase in the capacity of the ABS heat exchanger.

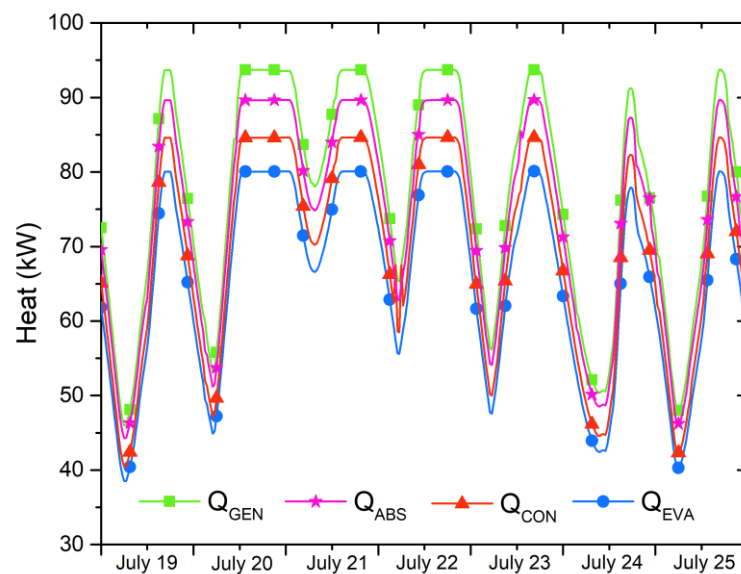


Figure 8. Operational performance of Q_{GEN} , Q_{EVA} , Q_{CON} , and Q_{ABS} heat exchangers during the critical summer week.

Figure 9 shows the heat transfer in EVA and fresh water production during the critical summer week. It can be seen that the increases in cooling capacity and fresh water production are proportional. This is because, as mentioned above, in order to meet the demand for cooling, it is necessary to control the production of steam (7) and bring it into the EVA to provide the cooling effect. This coolant flow, when suctioned by the ejector, is converted into product water, therefore, if the cooling capacity is increased, the product water also increases. The system operating at its maximum cooling capacity can satisfy a demand of 80 kW and a water production of 122 kg/h. During the week analyzed, a total production of 16.94 m³ was reached—while the average daily production of 2406 kg/day—enough to satisfy the daily water requirements of four people in a coastal hotel in Mexico [38] or to cover the basic services of 24 people according to World Health Organization (WHO) [39].

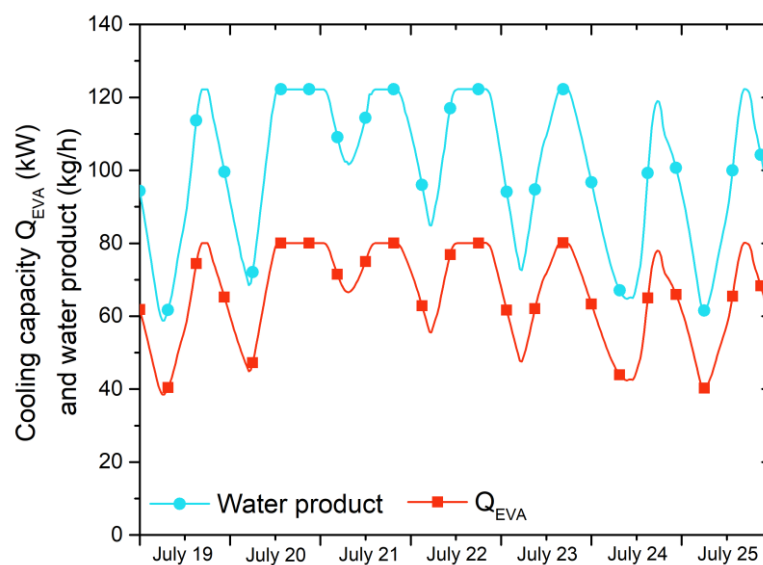


Figure 9. Behavior of cooling capacity and water product during the critical summer week.

Figure 10 shows the behavior of the cooling and desalination indicators, considered to evaluate the performance of the proposed hybrid system. It can be seen that the COP and the PR have a similar behavior, because both depend directly on the cooling demand. It is also observed that both indicators decrease when there is low cooling demand; this is because the decrease in cooling capacity implies less steam generation in the GEN, causing the high pressure in the GEN to decrease and the latent heat of the LiBr/H₂O solution to increase. Therefore, more heat is needed in the GEN to produce cooling steam. On the other hand, with low cooling capacities, the COP shows a greater decrease than the PR due to the energy consumption of the pumps. The average COP during the week of operation was 0.82, which is 13.88% higher than the COP reported in conventional single-effect LiBr/H₂O absorption-cooling systems. This is due to the use of three pressure levels, which allowed the ΔP between the GEN and the ABS to be reduced, allowing the EVA to reach adequate pressure levels for cooling. On the other hand, considering that the system can provide two services simultaneously, it can be seen that the maximum COP_G is 1.66, while the average COP_G is 1.64, being 2.27 times higher than the COP of conventional single-effect LiBr/H₂O absorption units. The system is capable of providing space cooling more efficiently than conventional systems, in addition to producing water with an average PR of 0.83.

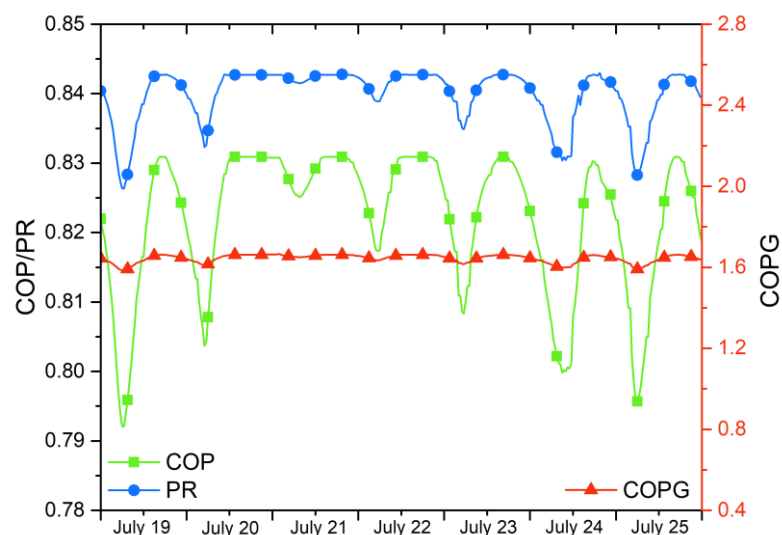


Figure 10. Performance of COP, COP_G, and PR indicators during the critical summer week.

3.3. Technological Considerations

The technological proposal analyzed in this work presents different challenges in terms of current technological development. The commercial maturity of solar heating and absorption systems is sufficient to be used in the current proposal, with simple modifications in the operating conditions. However, the main challenge is focused on the product water extraction and conditioning subprocess. At present, this type of system is not commercially available, so these components must first be developed so that they can work efficiently under the operating conditions mentioned in the study. Once the technological maturity of all the systems involved is achieved, their energy integration will be carried out in order to experimentally corroborate the results. On the other hand, given the nature of the system, an adequate application for the capacity of the equipment must be sought, where sufficient energy resources are available: in this case, high levels of solar radiation. As it is a thermal machine, the capacity–cost ratio can be fundamental. At lower capacity, the specific cost of the system can be increased as with other technologies, such as power cycling and vapor compression cooling systems. However, this will be analyzed in detail in future work, when the main components of the system will be further developed.

4. Conclusions

A novel solar hybrid system of LiBr/H₂O absorption cooling and flash seawater desalination was proposed. This system couples a single-effect absorption-cooling open-cycle with three pressure levels, thus allowing an internal energy and mass integration with a single-stage flash-desalination process, producing simultaneously cooling and drinking water. A solar thermal collector field and a TEST are used to generate the thermal energy required for its activation. Its operation is analyzed under the dynamics of a case study of a 20-room hotel complex in the city of San Felipe, Baja California, Mexico, where the influence of the solar resource, ambient temperature and cooling demand was studied.

The proposed novel system was evaluated during the summer period and in the week of highest cooling requirement. The absorption-cooling subprocess, using three levels of pressure, presented an increase of 13.88% in the average COP, compared to conventional LiBr/H₂O absorption systems. Also, considering that the system provides cooling and desalination simultaneously, it has an average COP_G of 1.64, being 2.27 times higher than the COP of conventional LiBr/H₂O absorption units of single-effect.

The system, during the critical week, presented a production of desalinated water of 16.94 m³ with an average PR of 0.83; while the average daily production of product water was 2406 kg/day, enough to satisfy the daily water requirements of four people in a Mexico hotel or to cover the basic services of 24 people according to the WHO. The dimensioning of the solar thermal collector field and TEST resulted in a total collection area of 620 m² with 30 m³ of storage in the form of sensible heat. This resulted in a solar fraction of 69% requiring an extra 53 MWh of auxiliary energy to meet the thermal energy requirements.

Author Contributions: Conceptualization, J.A.A.-J. and R.L.-Z.; methodology, N.V.-L. and L.H.-C.; software, J.A.A.-J., R.L.-Z., and J.R.-A.; validation, R.L.-Z.; formal analysis, S.O.-B.; investigation, N.V.-L. and L.H.-C.; resources, N.V.-L.; writing—original draft preparation, J.A.A.-J. and R.L.-Z.; writing—review and editing, N.V.-L. and L.H.-C.; supervision, S.O.-B.; project administration, N.V.-L.; funding acquisition, N.V.-L. All authors have read and agreed to the published version of the manuscript.

Funding: This research received no external funding.

Acknowledgments: The authors acknowledge CONACYT for the support received through a graduate scholarship for Jesús Armando Aguilar-Jiménez and the Center for Renewable Energy Studies, Engineering Institute, Autonomous University of Baja, California. The authors also acknowledge the CYTED Thematic Network “CIUDADES INTELIGENTES TOTALMENTE INTEGRALES, EFICIENTES Y SOSTENIBLES (CITIES)” no 518RT0558.

Conflicts of Interest: The authors declare no conflict of interest.

Abbreviations

GEN	Generator
ABS	Absorber
CON	Condenser
EVA	Evaporator
HX1	Recovery heat exchanger
HX2	Driving fluid cooler
AUX	Auxiliary heat exchanger
TEST	Thermal energy storage tank
SFP	Solar fluid pump
HWP	Hot water pump
SP	Solution pump
SWP	Seawater pump
SWP1	Seawater pump for cooling
EP	Ejector pump
SV	Solution valve
RV	Refrigeration valve

SWV	Seawater expansion valve
DIV	Streams divisor
SEP	Separator equipment
EJE	Ejector
BC1	Ejector barometric column
BC2	Separator barometric column
PWT	Product water tank
BRC	Brine container
COP	Coefficient of operation
PR	Performance ratio
PW	Product water

Nomenclature

T	Temperature [°C]
P	Pressure [kPa]
Q	Heat transfer [kW]
ASC	Solar collection area
GT	Incident solar radiation in the collector opening area
a_0	Optical efficiency of the solar collector
a_1	First order efficiency coefficient
a_2	Second order efficiency coefficient
T_{in}	Collector inlet temperature
T_a	Ambient temperature
f	Solar fraction
E_f	Thermal efficiency of solar collectors

Subscripts

a	Ambient
in	Inlet
1,2,3...	Number of streams
sf	Solar field

References

1. EIA Annual Energy Outlook 2020 with Projections to 2050; Energy Information Administration: Washington, DC, USA, 2020.
2. Chowdhury, T.; Mokheimer, E.M.A. Recent developments in solar and low-temperature heat sources assisted power and cooling systems: A design perspective. *J. Energy Resour. Technol.* **2020**, *142*, 040801. [[CrossRef](#)]
3. Nassrullah, H.; Anis, S.F.; Hashaikeh, R.; Hilal, N. Energy for desalination: A state-of-the-art review. *Desalination* **2020**, *491*. [[CrossRef](#)]
4. Castro, M.; Alcanzare, M.; Esparcia, E.; Ocon, J. A Comparative Techno-Economic Analysis of Different Desalination Technologies in Off-Grid Islands. *Energies* **2020**, *13*, 2261. [[CrossRef](#)]
5. Ghaffour, N.; Missimer, T.M.; Amy, G.L. Technical review and evaluation of the economics of water desalination: Current and future challenges for better water supply sustainability. *Desalination* **2013**, *309*, 197–207. [[CrossRef](#)]
6. Azinheira, G.; Segurado, R.; Costa, M. Is renewable energy-powered desalination a viable solution for water stressed regions? A case study in Algarve, Portugal. *Energies* **2019**, *12*, 4651. [[CrossRef](#)]
7. Omar, A.; Nashed, A.; Li, Q.; Leslie, G.; Taylor, R.A. Pathways for integrated concentrated solar power - Desalination: A critical review. *Renew. Sustain. Energy Rev.* **2020**, *119*, 109609. [[CrossRef](#)]
8. Al-Karaghoul, A.; Kazmerski, L.L. Energy consumption and water production cost of conventional and renewable-energy-powered desalination processes. *Renew. Sustain. Energy Rev.* **2013**, *24*, 343–356. [[CrossRef](#)]
9. Mito, M.T.; Ma, X.; Albuflasa, H.; Davies, P.A. Reverse osmosis (RO) membrane desalination driven by wind and solar photovoltaic (PV) energy: State of the art and challenges for large-scale implementation. *Renew. Sustain. Energy Rev.* **2019**, *112*, 669–685. [[CrossRef](#)]

10. Ghaffour, N.; Bundschuh, J.; Mahmoudi, H.; Goosen, M.F.A. Renewable energy-driven desalination technologies: A comprehensive review on challenges and potential applications of integrated systems. *Desalination* **2015**, *356*, 94–114. [[CrossRef](#)]
11. Saikia, K.; Vallès, M.; Fabregat, A.; Saez, R.; Boer, D. A bibliometric analysis of trends in solar cooling technology. *Sol. Energy* **2020**, *199*, 100–114. [[CrossRef](#)]
12. Mohammadi, K.; Saghafifar, M.; Ellingwood, K.; Powell, K. Hybrid concentrated solar power (CSP)-desalination systems: A review. *Desalination* **2019**, *468*, 114083. [[CrossRef](#)]
13. Inayat, A.; Raza, M. District cooling system via renewable energy sources: A review. *Renew. Sustain. Energy Rev.* **2019**, *107*, 360–373. [[CrossRef](#)]
14. Chandrashekara, M.; Yadav, A. Water desalination system using solar heat: A review. *Renew. Sustain. Energy Rev.* **2017**, *67*, 1308–1330. [[CrossRef](#)]
15. Ullah, I.; Rasul, M.G. Recent developments in solar thermal desalination technologies: A review. *Energies* **2019**, *12*, 119. [[CrossRef](#)]
16. Ahmed, F.E.; Hashaikeh, R.; Hilal, N. Solar powered desalination—Technology, energy and future outlook. *Desalination* **2019**, *453*, 54–76. [[CrossRef](#)]
17. Aguilar-Jiménez, J.A.; Velázquez, N.; López-Zavala, R.; González-Uribe, L.A.; Beltrán, R.; Hernández-Callejo, L. Simulation of a Solar-Assisted Air-Conditioning System Applied to a Remote School. *Appl. Sci.* **2019**, *9*, 3398. [[CrossRef](#)]
18. Aguilar-Jiménez, J.A.; Velázquez-Limón, N.; López-Zavala, R.; González-Uribe, L.A.; Islas, S.; González, E.; Ramírez, L.; Beltrán, R. Optimum operational strategies for a solar absorption cooling system in an isolated school of Mexico. *Int. J. Refrig.* **2020**, *112*, 1–13. [[CrossRef](#)]
19. Byrne, P.; Fournaison, L.; Delahaye, A.; Ait Oumeziane, Y.; Serres, L.; Loulergue, P.; Szymczyk, A.; Mugnier, D.; Malaval, J.L.; Bourdais, R.; et al. A review on the coupling of cooling, desalination and solar photovoltaic systems. *Renew. Sustain. Energy Rev.* **2015**, *47*, 703–717. [[CrossRef](#)]
20. Anand, B.; Murugavel, S. Performance analysis of a novel augmented desalination and cooling system using modified vapor compression refrigeration integrated with humidification-dehumidification desalination. *J. Clean. Prod.* **2020**, *255*, 120224. [[CrossRef](#)]
21. Qasem, N.A.A.; Zubair, S.M.; Abdallah, A.M.; Elbassoussi, M.H.; Ahmed, M.A. Novel and efficient integration of a humidification-dehumidification desalination system with an absorption refrigeration system. *Appl. Energy* **2020**, 263. [[CrossRef](#)]
22. Kerme, E.D.; Orfi, J.; Fung, A.S.; Salilih, E.M.; Khan, S.U.D.; Alshehri, H.; Ali, E.; Alrasheed, M. Energetic and exergetic performance analysis of a solar driven power, desalination and cooling poly-generation system. *Energy* **2020**, 196. [[CrossRef](#)]
23. Sahoo, U.; Kumar, R.; Pant, P.C.; Chaudhury, R. Scope and sustainability of hybrid solar-biomass power plant with cooling, desalination in polygeneration process in India. *Renew. Sustain. Energy Rev.* **2015**, *51*, 304–316. [[CrossRef](#)]
24. Alelyani, S.M.; Fette, N.W.; Stechel, E.B.; Doron, P.; Phelan, P.E. Techno-economic analysis of combined ammonia-water absorption refrigeration and desalination. *Energy Convers. Manag.* **2017**, *143*, 493–504. [[CrossRef](#)]
25. Mohammadi, K.; McGowan, J.G. An efficient integrated trigeneration system for the production of dual temperature cooling and fresh water: Thermoeconomic analysis and optimization. *Appl. Therm. Eng.* **2018**, *145*, 652–666. [[CrossRef](#)]
26. Calise, F.; Dentice d’Accadia, M.; Piacentino, A.; Vicidomini, M. Thermoeconomic optimization of a renewable polygeneration system serving a small isolated community. *Energies* **2015**, *8*, 995–1024. [[CrossRef](#)]
27. Calise, F.; Macaluso, A.; Piacentino, A.; Vanoli, L. A novel hybrid polygeneration system supplying energy and desalinated water by renewable sources in Pantelleria Island. *Energy* **2017**, *137*, 1086–1106. [[CrossRef](#)]
28. Jabari, F.; Nazari-heris, M.; Mohammadi-ivatloo, B.; Asadi, S.; Abapour, M. A solar dish Stirling engine combined humidification-dehumidification desalination cycle for cleaner production of cool, pure water, and power in hot and humid regions. *Sustain. Energy Technol. Assessments* **2020**, *37*, 100642. [[CrossRef](#)]
29. López-Zavala, R.; Velázquez-Limón, N.; González-Uribe, L.A.; Aguilar-Jiménez, J.A.; Alvarez-Mancilla, J.; Acuña, A.; Islas, S. A novel LiBr/H₂O absorption cooling and desalination system with three pressure levels. *Int. J. Refrig.* **2019**, *99*, 469–478. [[CrossRef](#)]

30. López-Zavala, R.; Velázquez, N.; González-Uribe, L.A.; Quezada-Espinoza, K.M.; Aguilar-Jiménez, J.A.; Islas, S.; Nakasima-López, M.; González, E. Absorption cooling and desalination system with a novel internal energetic and mass integration that increases capacity and efficiency. *Desalination* **2019**, *417*, 114144. [[CrossRef](#)]
31. *AHRI Standard 560–2000 for Absorption water Chilling and Water Heating Packages*; Air-Conditioning, Heating, and Refrigeration Institute: Arlington, TX, USA, 2000.
32. Mejía Mercado, B.E.; Hinojosa Corona, A.; Hendrickx, M.E. *Explorando el Mar Profundo del Golfo de California 2008–2014*; CICESE: Ensenada, Mexico, 2014; ISBN 978-607-95688-1-8.
33. Zheng, H. Chapter 1—General Problems in Seawater Desalination. In *Solar Energy Desalination Technology*; Elsevier: Amsterdam, The Netherlands, 2017; pp. 1–46, ISBN 9780128054116.
34. Florides, G.A.; Kalogirou, S.A.; Tassou, S.A.; Wrobel, L.C. Design and construction of a LiBr-water absorption machine. *Energy Convers. Manag.* **2003**, *44*, 2483–2508. [[CrossRef](#)]
35. Kahraman, N.; Cengel, Y.A. Exergy analysis of a MSF distillation plant. *Energy Convers. Manag.* **2005**, *46*, 2625–2636. [[CrossRef](#)]
36. Palenzuela, P.; Hassan, A.S.; Zaragoza, G.; Alarcón-Padilla, D.C. Steady state model for multi-effect distillation case study: Plataforma Solar de Almería MED pilot plant. *Desalination* **2014**, *337*, 31–42. [[CrossRef](#)]
37. Zheng, H. Chapter 7—Solar Desalination System Combined with Conventional Technologies. In *Solar Energy Desalination Technology*; Elsevier: Amsterdam, The Netherlands, 2017; pp. 537–622, ISBN 978-0-12-805411-6.
38. Bartram, J.; Howard, G. *Domestic Water Quantity, Service Level and Health*; World Health Organization: Geneva, Switzerland, 2003.
39. Becken, S. Water equity—Contrasting tourism water use with that of the local community. *Water Resour. Ind.* **2014**, *7–8*, 9–22. [[CrossRef](#)]



© 2020 by the authors. Licensee MDPI, Basel, Switzerland. This article is an open access article distributed under the terms and conditions of the Creative Commons Attribution (CC BY) license (<http://creativecommons.org/licenses/by/4.0/>).